Unisanta Science and Technology, **2019, 3, December**
Published Online 2019 Vol.8 N°2 http://periodicos.unisanta.br/index.php/sat)

UNISANTA
Science and Technology
ISSN 2317-1316

Impact of Welding Consumables Strength Level on Metallurgical and Mechanical Properties Homogeneity of Welds Obtained with a Complex Phase Steel

Patrícia Pala Diniz[1,2], Willy Ank de Morais[1,3]

UNISANTA[1] - Universidade Santa Cecília - Programa de Pós-Graduação em Engenharia Mecânica - PPGEMec
Rua Oswaldo Cruz, 266. 11045-100, Santos-SP, Brasil.

USIMINAS - CUBATÃO[2] - Usinas Siderúrgicas de Minas Gerais - Gerência de Qualidade
Rod. Dom Domênico Rangoni, s/n - Jardim das Indústrias. 11573-900, Cubatão, São Paulo, Brasil.

WILLY ANK SOLUÇÕES[3]
Rua Onze de Junho, 316 A.102. 1130-160, São Vicente, São Paulo, Brasil.
E-mail*:* patricia.pala@usiminas.com
Received November, 2019

Abstract: There has been an increase in Advanced High-Strength Steels (AHSS) use in the automotive industry, including Complex-Phase (CP) steels that have a good combination of strength and ductility. However, despite the potential benefits of its higher mechanical strength (800 MPa), autoparts manufactured of CP steel are submitted to welding process with consumables with much lower level of mechanical strength. In order to offer an option to rationalize the use of this material in terms of welded joint, it were investigated joint performance of a pulsed GMAW welding process using ER70S-6 (class 70 psi or 482 MPa UTS) and ER110S-G (class 110 psi or 760 MPa UTS) consumables to join samples of CP-800 hot rolled steel (class 800 MPa UTS) with the same welding commercial parameters used nowadays. For this they were performed tensile, impact, hardness and metallographic tests in adequate welding samples. The results obtained in this work point to a better performance by using the ER110S-G consumable, but due to the lack of penetration in 4.0 mm thick plates it is recommended to use this consumable, under the same conditions of consumable welding ER70S-6 only on sheets up to 2.0 mm.

Keywords: AHSS steels, Complex Phase Steel, pulsed GMAW, autoparts, welding joints.

1. Introduction

In the automotive industry, there is a strong demand for vehicle weight reduction, increased passenger safety, reduced CO_2 emissions and fuel economy. In addition to the new global standards for emissions and fuel economy, consumers are demanding safer cars, and governments are responding with new tests and standards. To achieve these objectives, it was necessary to migrate from the traditionally used steels (MARRA, 2008).

One way to achieve this goal is by the use of advanced high-strength steels (AHSS), as suggest by Figure 1. These steels have been in use for a number of years since the beginning of their development in the mid-1990s (Keller et al., 2015). The AHSS family includes Dual Phase (DP), Complex-Phase (CP), Ferritic-Bainitic (FB), Martensitic (MART), Transformation Induced Plasticity (TRIP), among others specials steels. The main difference between conventional high strength steels (HSS) and advanced high strength steels (AHSS) is found in their microstructures, that differs from the traditional ferrite-perlite. The special microstructure of the AHSS gives more strength and toughness to these steels, positively impacting, for example, the crash test results of automobiles. The evolution perceived over more than a decade of crash test with the Fiat Punto automobile, as showed by Fig. 1, can be associated, among other modern car design conditions, with the increasing use of AHSS.

One of these steels is the Complex-Phase (CP) steels, which stands out for having a good combination of high strength and ductility. Its microstructure consists of an aggregate of several phases, being that its base matrix is composed of ferrite and bainite, with very fine granulation. Furthermore, there are present other metallurgical phases in residual quantities: martensite, constituent MA (martensite - austenite), perlite and retained austenite. Because this steel is normally microalloyed to titanium,

Copyright © 2019 ISESC.

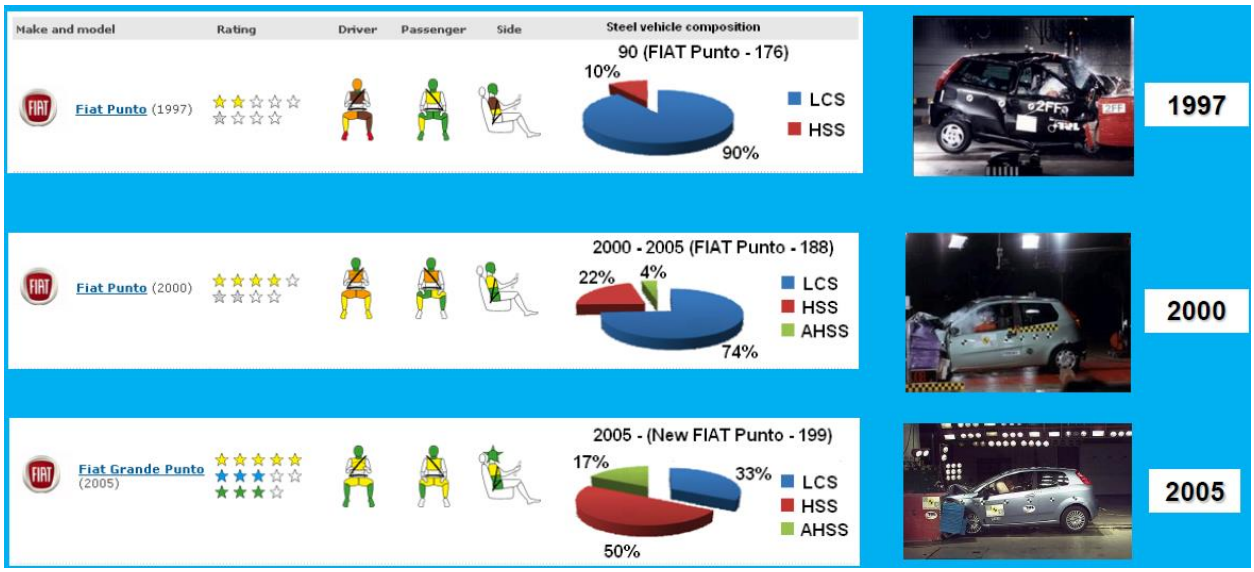


Figure 1. Results of EURONCAP crash test assessments against the evolution of steels (FERREIRA, 2016).

niobium, vanadium, molybdenum, boron and/or chromium, it has fine and stable carbides in its structure, too.

The CP is available on the market as hot and cold rolled formed. These steels are applied in the automotive industry, as bumpers, door security bars, B columns, automotive suspension parts, among others. As a common point in these applications, the necessity of the material gives to the autopart sufficient integrity for guarantee the safety of passengers during an accident or collision event.

Normally, steel autoparts are submitted to welding operations, during its manufacture. These operations have with high potential of altering microstructures, especially the complex ones. Due this, it is essential to understanding the effect of welding on the microstructures of AHSS to adjust their use to autoparts.

Cardenas et al. (2015) presented a work about the effect of GMAW welding on the tensile properties of a hot-rolled complex phase 780 steel. In the first phase of their study, the different transfer methods were compared using the AWS 5.18 (2001) ER70S-6 consumable; pulsed, CMT (Cold Metal Transfer), CMT-Twin (two solder sources) and short circuit. The conclusion was that the best welding efficiency was by the pulsed transfer mode, with the rupture in traction occurring in the ZTA. In addition, the material welded by the process of the pulsed GMAW with ER70S-6 presented greater reduction of hardness in the ZTA, but not exceeding 9%.

In the second phase of Cardenas et al. (2015) study, using only pulsed robotic GMAW process, it was compared welding consumables with different mechanical strength levels: 70, 90 and 110 ksi. In that study, the conclusion was that there was a change in the rupture site of the samples. For welds obtained with high strength level consumables (90 and 110 ksi), rupture occurred in the hot affect zone (HAZ). On the other hand, using lower level strength consumable (70 ksi), rupture was observed in the base metal (BS).

Similar works developed with the DP and TRIP steels (Burns, 2009 and Kapustka et al., 2008), present different conclusions from those obtained as the CP steel, therefore, as quoted by Mesplont (2002) and Cardenas et al. (2015), further work should be developed to evaluate the effects of welding processes on CP steels.

Despite all the studies carried out since 2000's begins, the automotive industry still employs lower strength level ER70S-6 grade consumables in GMAW robotic welding of autoparts made of CP steel. ER70S-6 grade exhibit minimum ultimate tensile strength (UTS) of 70 ksi (480 MPa) according AWS A5.18 / A5.18M (2001) in contrast to a UTS at least 780 MPa for CP steels (Marra, 2008). Therefore, the minimum tensile strength of the base metal (CP) is approximately 60% above the strength of the consumable used in the welding.

Therefore, this study aimed to evaluate two welding conditions of a CP steel, development by Usiminas as USI-CP 800 (UTS ≥ 113 ksi). For this purpose, the standard consumable, ER70S-6 (UTS ≥ 80 ksi), and a higher strength consumable, ER110S-G (UTS ≥ 110 ksi) were used, this last more mechanically similar to the USI-CP 800 steel studied. Due to the practice of the

Copyright © 2019 ISESC.

automobile industry, which generally employs GMAW robotic welding in auto parts and for what has been pointed out in the literature (Cardenas et al., 2015, Burns, 2009 and Kapustka et al., 2008), this work has adopted the pulsed robotic GMAW welding process.

2. Materials and Methods

The study focused on the impact of the welding process using a CP steel, for autoparts application, developed by USIMINAS-Cubatão as USI-CP 800 4.00 mm thick, hot rolled and pickled. Such steel is intended to meet the requirements of the European specification EN 10338 (2015), which specifies uncoated hot rolled complex phase steels. Table 1 shows the values of mechanical properties required for this material and Table 2 the chemical requirements as hot rolled. Square samples with 300×300 mm size were taken from a hot-rolled coil from 2000 mm of its end, in order to avoid a non-representative region of the material.

The choice of the welding conditions was based as appointed by two large companies in the automobile industry, denominated in this work as "A" and "B". This choice was done to facilitate the incorporation of the results of this study, reducing the technological impacts, to the current conditions practiced in the manufacture of the auto parts. These companies actually use both CP steel and pulsed GMAW robotized welding process as summarized in Table 3 The wire feed speed adopted, after practical tests, was 8 m/min., a voltage of 21.6 V, and a current of 205 A.

The consumables employed in this study were supplied by Voestalpine Böhler Welding Welds of Brazil Ltda., as presented and described in Table 4. In this work the manufacturer's recommendations (Böhler, 2017) were adopted for consumables used with 1.2 mm diameter: voltage from 17 to 30 V and current from 150 to 320 A. Through a partnership, Fronius International made available its development center a Fronius TPS/i® welding machine, a FANUC ARC Mate OiB® specialist

Table 1. Mechanical properties required for USI-CP 800 steel.

YS, MPa (ksi)	UTS, MPa (ksi)	%Elong. L_o= 80 mm (%)	Test direction
680 to 780 (100 to 110)	780 to 960 (110 to 140)	≥ 10	Transversal

Note: ksi values were approximate for rounding to nearest 10.

Table 2. Chemical composition required for USI-CP 800 steel.

%C	%Mn	%Si	%P	%S	%Cu	%(Nb+Ti+V)	%Al	%V	%B
≤ 0.18	≤ 2.20	≤ 1.20	≤ 0.040	≤ 0.015	≤ 0.20	≤ 0.17	≤ 1.20	≤ 0.20	≤ 0.005

Table 3. Parameters of CP steel welding process employed by two automotive companies in Brazil.

Reference Company	Process	Consumable AWS 5.18 (2001)	Diameter of consumable (mm)	Protection gas (Ar-CO_2)
A	Pulsed GMAW	ER-70S-6	1.2	85%-15%
B	Pulsed GMAW	ER-70S-6	1.0	92%-8%

Table 4. Characteristics of the consumables used in this work.

Material	Chemical composition		Mechanical Properties (typical)
standard: AWS 5.18 (**2001**) **designation**: ER70S-6 **Specification**: Böhler EMK 6D	0.08%C 0.90%Si 1.45%Mn		YS = 440 MPa UTS = 530 MPa %Elong. = 28% CVN = 110 J @ -30ºC
standard: AWS 5.28 (**2005**) **designation**: ER110S-G **Specification**: Böhler X 70-I	0.10%C 0.60%Si 1.60%Mn	0.25%Cr 0.25%Mo 1.30%Ni 0.10%V	YS = 800 MPa UTS = 900 MPa %Elong. = 19% CVN = 47 J @ -50ºC

Copyright © 2019 ISESC.

robotic arm and a welding operator to perform samples welding. In the pulsed GMAW welding process of all the samples a mixture of 92% argon gas and 8% CO_2 was used. As practiced in the automotive industry, the welded joints were butt square edge type, thus not beveled at all.

In order to analyze what were the characteristics of USI-CP 800 steel welded and un-welded with ER70S-6 and ER110S-G consumables, chemical, tensile, and hardness tests were carried out as well metallography analysis. Tensile test specimens obtained from rough steel coil samples, without welding, were made according to ASTM A370 (2017), in both the transverse and longitudinal direction of rolling. For the evaluation of welded joints, after preparation and etching, the metallographic aspect was recorded through images obtained from a metallographic microscope and analyzed by Photoshop CC software. After metallographic recorded, Vickers hardness (HV_3) tests were performed in welded region, including base metal, hot affect and fused zones (BM, HAZ and FS). It was used a load of 3 kgf and 0.6 mm spacing between each measurement point.

In addition, weldability of CP steel is not limited by the formation of fragile (non-ductile) phases, but by diffused based changes in the present phases, as described by Mesplont (2002). That change reduces the mechanical strength and probably the toughness of these phases, compromising the mechanical performance of the CP steel. Hence the automotive industry's practice of adopting a weld bead with higher reinforcement or bead height, leaves the need, in this study, to evaluate this geometry via Finite Element Method (FEM). Then, the specimens of the welded samples were prepared maintaining the weld reinforcement (WR), simulating the conditions of actual use in the autoparts. The evaluation of the influence of an unplanned weld bead was done through SolidWorks® Simulator software.

3. Results and Discussion

Figure 2 and Figure 3 exemplify the conditions of the welded joints obtained in this study using the consumables ER70S-6 and ER110S-G. With the same welding parameters, the use of the ER110S-G consumable takes a weld joint with loss of penetration, a type of result that would be expected, since consumable materials are different (see Table 4). Clearly, the welding parameters must be adjusted accordingly, to allow 100% joint penetration using ER110S-G consumable. One way to do this is by increasing the ratio argon/carbon dioxide share in the blend. In addition, welding with the ER110S-G was more stable, resulting in less welding spatter compared to the ER70S-6.

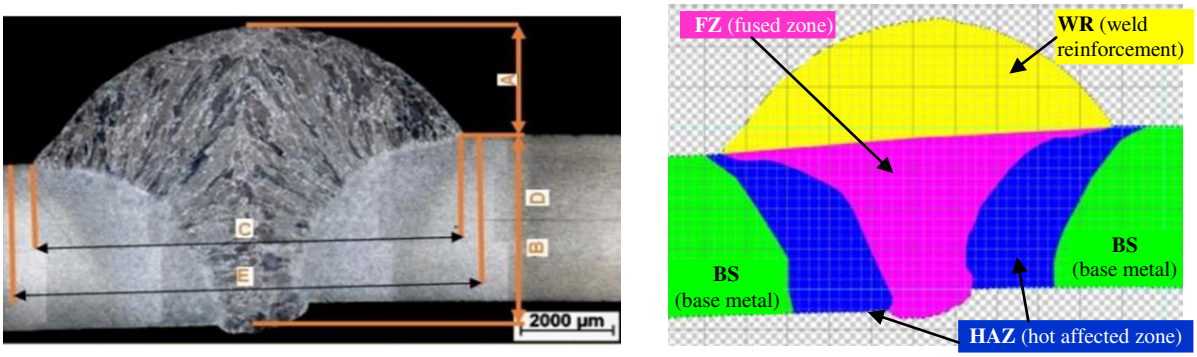


Figure 2. Example of weld profile evaluation of a CP steel sample welded with a ER70S-6 consumable.

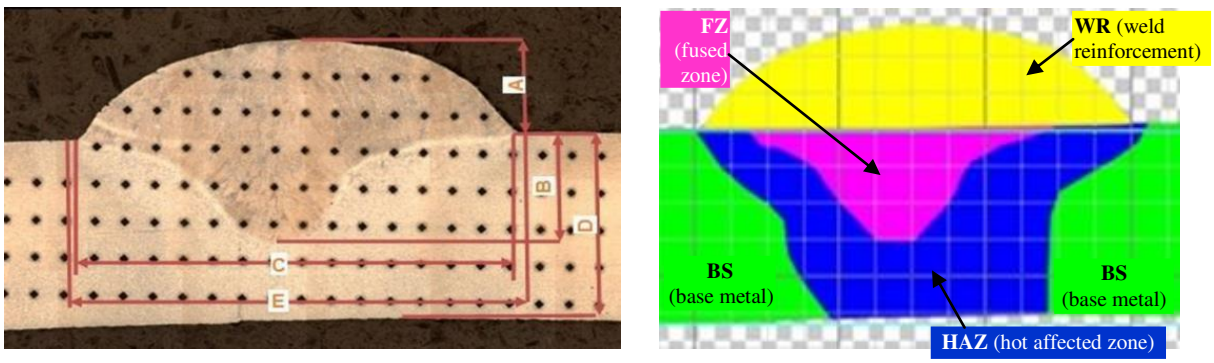


Figure 3. Example of weld profile evaluation of a CP steel sample welded with a ER110S-G consumable.

Copyright © 2019 ISESC.

Table 5 presents the average dimensions measured by the image analysis software. These dimensions are represented in the Figures 2 and 3 by the letters "A" to "E". Analyzing the metallographies by Photoshop software, were obtained the relative areas A1 and A2, and used to calculate the welding dilution (δ), as calculated by Equation (1):

$$\delta = \frac{A2}{A1}(\times 100\%) \quad (1)$$

Where area A1 represents the total melted region of the weld, formed by base metal (FZ, Fig. 2 and 3) and consumables (WR, Fig. 2 and 3). Besides, the area A2 quantifies the fused zone area formed only by the melting of consumable (WR, Fig. 2 and 3).

voltage values, or more than one pass, to obtain full penetration and weld service of the strength characteristics of the base metal.

A larger weld reinforcement increases the thickness of the joint, reducing the local stress, and thus preventing rupture to occur even with a lower strength developed after welding. But, by the other side, it can also generate a stress concentrator. To assess this stress concentration during tensile loading, the Von Mises equivalent stress distribution of a tensile test sample was calculated, as shown in Figure 4 with and without weld reinforcement. The performance of the weld reinforcement with the ER70S-6 consumable was evaluated considering a base material thickness of 4 mm (B, Tab. 5) and a reinforcement with a height of 3.10 mm (A, Tab. 5), so that in this region the total thickness was 7.10 mm.

Table 5. Dimensions and dilutions of weld beads geometries obtained by consumables type.

Dimension type (see Fig. 2 and 3)		ER70S-6	ER110S-G
A	Reinforcement height	3.1 mm	2.1 mm
B	Penetration	4.0 mm	2.1 mm
C	Bead width	9.0 mm	9.0 mm
D	HAZ height	4.0 mm	4.0 mm
E	HAZ width	10.2 mm	9.3 mm
δ	Dilution (according Eq. 1)	42%	35%

Table 6. Results of tensile tests on welded specimens of USI-CP 800 steel.

Condition		YS, MPa (ksi)	UTS, MPa (ksi)	%Elong. L_0=50 mm	YS/UTS
Base Metal		738 (107)	810 (117)	19%	0.91
Welding with ER70S-6	with reinf.	765 (111)	809 (117)	12%	0.95
	without reinf.	583 (85)	703 (102)	6%	0.83
Welding with ER110S-G	with reinf.	384 (56)	495 (72)	4%	0.77
	without reinf.	400 (58)	403 (58)	5%	0.99
USI-CP 800 (steel requirements)		680 to 780 (98 to 113)	780 to 960 (113 to 139)	>10%	–

Table 6 shows the average tensile results obtained with samples welded with the consumable ER70S-6 and ER110S-G, with and without removal of the weld reinforcement (WR, see Fig. 2 and 3). Only the standard condition with the ER70S-6 consumable and the maintenance of the large reinforcement area were able to meet the mechanical strength requirements expected in the base metal (USI-CP 800). Despite the higher theoretical resistance of the joint obtained by the ER110S-G consumable, it did not present adequate penetration in the conditions currently practiced by the industry (Tab. 5) to provide the desired strength. For this, the procedure should be changed, either by gas mixing, current and

In the specimen with the weld reinforcement it was possible to observe a higher concentration of stresses around the base of the bead. In the flat specimen, that is, with the weld reinforcement (WR) mechanically obliterated (rectified), this stress concentrator is eliminated.

As observed by Figure 7, the stresses concentrated at the base of the weld bead (453 MPa) are practically twice the stresses present in the rest of the useful section of the specimen (226 MPa), away from the region of the stress concentrator. Therefore, it is expected that the specimens with the weld reinforcement, when subjected to the tensile test, will undergo plastic deformation and fracture in the region with the highest stress concentration,

Copyright © 2019 ISESC.

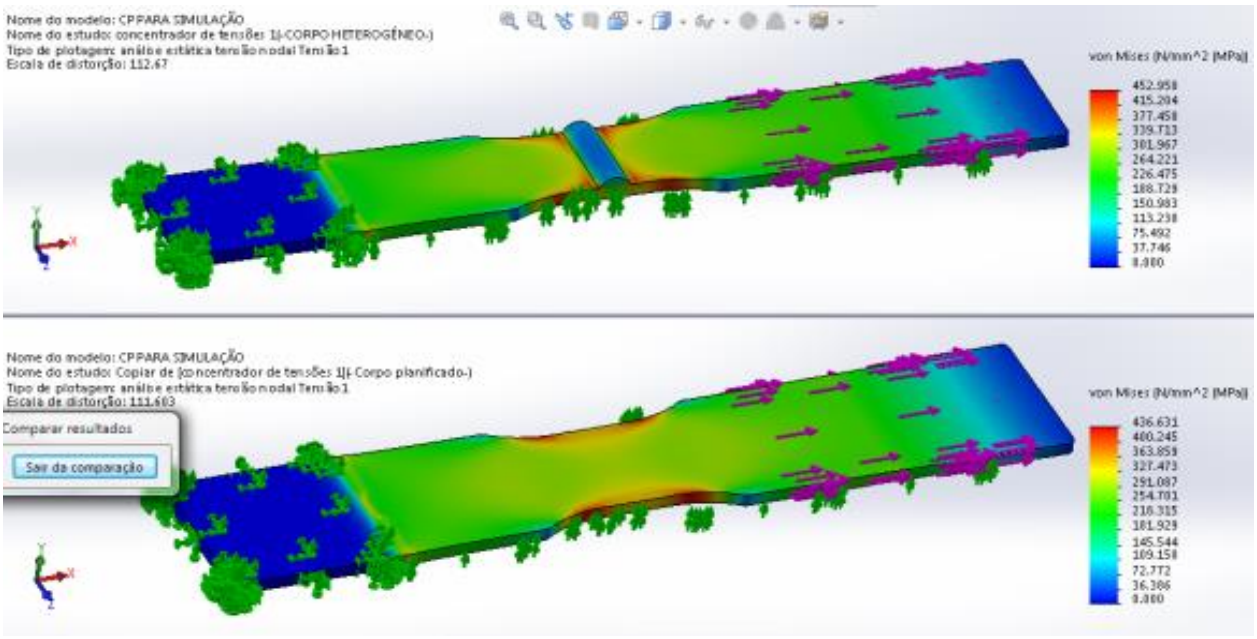


Figure 4. Comparison of stress distributions between a tensile test specimen with and without a weld bead.

at the base of the weld bead reinforcement, in the edge of the specimen. This, in fact, was what happened in the unflatted samples of this study. As the material is relatively ductile, it can deform locally, reducing the stress concentration and, at the end, presenting a mechanical resistance compatible with the base metal if a large weld reinforcement (WR) is present.

However, under fatigue conditions, this region can cause cracks much more easily, compromising not only the strength of the component but also the safety of the vehicle's occupants under these conditions.

For hardness analysis were made 139 and 219 measurements on welded joint composed by ER70S-6 and ER110S-G consumables, respectively. The measurement conditions and results are shown in Figure 5.

In the case of joints obtained with the consumable ER70S-6 (left, Fig. 5), the hardness obtained for the base metal was around 280 HV_3. In some places a higher hardness was found, 320 HV_3, probably due to the presence of martensite. In the other regions where the presence of bainite was predominantly observed by Scanning Electron Microscopy (SEM).

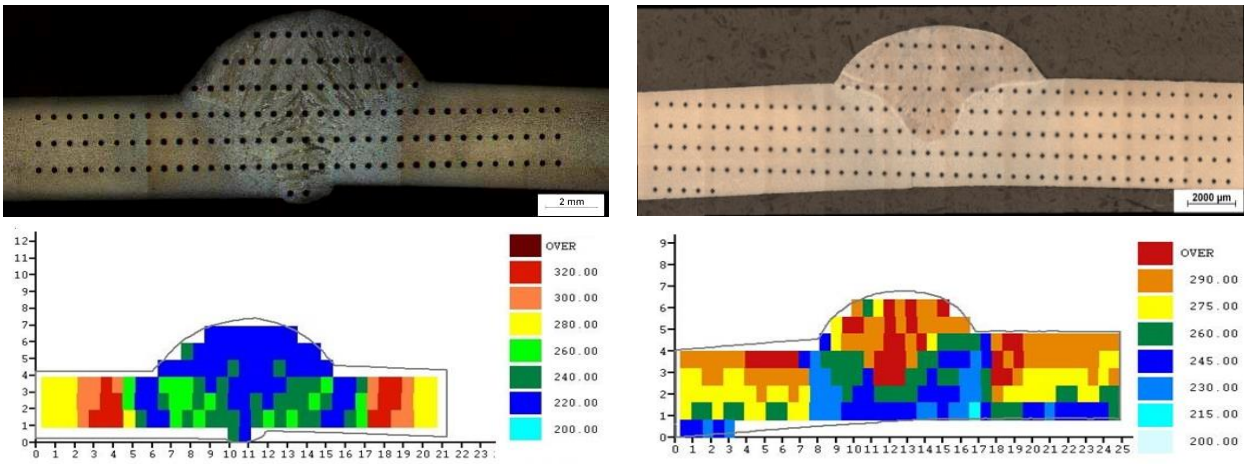


Figure 5. Hardness mapping performed on USI-CP 800 samples welded through the pulsed GMAW process with the ER70S-6 (left) and ER110S-G (right) consumables.

Copyright © 2019 ISESC.

Although the penetration of the weld was only partial in this work, by the use of ER110S-G consumable was partial, it is possible to evaluate and draw some important conclusions considering the hardness results obtained in this welded joint (right, Fig. 5). The region of the fused zone, which is the region basically formed by the filler metal (consumable), presented the greatest hardness, as obtained in the mapping. Observed hardness equal to or greater than 290 HV is reasonable, since the consumable used has a resistance of 900 MPa (130 ksi) and chemical elements that increase its hardenability, such as Cr, Ni and Mo (see Tab. 4). As expected, the conclusion was the same as that presented in the work by Cardenas et al. (2015), the greater the resistance of the consumable used, the greater the average hardness of the weld.

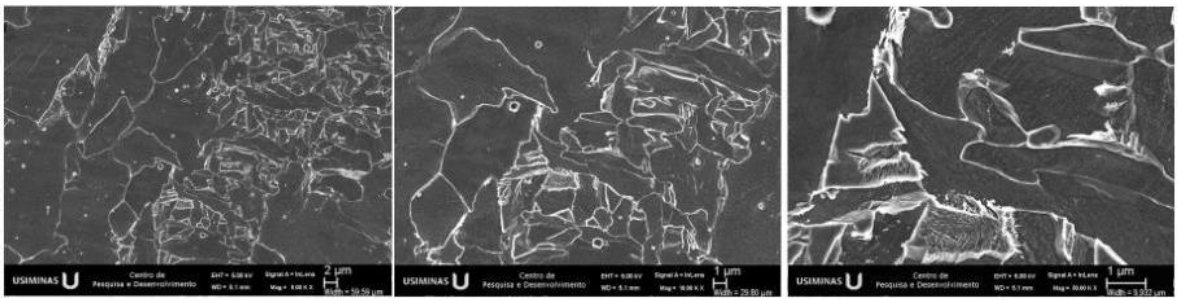
The lower value of hardness mapped by the consumable with the highest resistance was 220 HV_3, and 202 HV_3 with the consumable ER70S-6. Thus, the hardness change in the joint is less abrupt in the former consumable (ER110S-G). Depending on the effort that the material undergoes, the rupture must occur in the region of least hardness. In the case of the ER110S-G consumable, as it has a hardness similar or superior to that of the base metal, at rupture, it must occur in the ZTA and not in the weld. However, other factors, such as the weld geometry, can cause rupture in another region by other mechanisms (example: fatigue).

Scanning electron microscopy (SEM) was used to verify the change in the microstructure after the welding process. The need to use the SEM is due to the fact that the microstructure of the welded joint and the base metal (USI-CP 800) are extremely fine (average grain size about 5 μm).

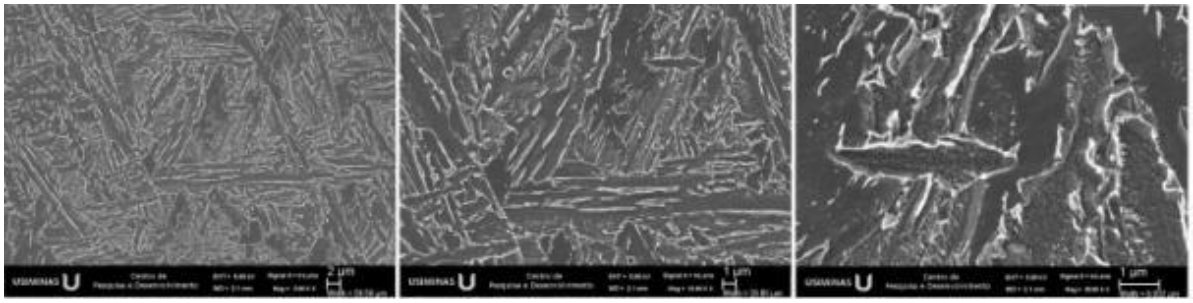
In the base metal, it is possible to observe microstructure of fine-grained ferrite with a second phase that promotes a higher hardness than in HAZ, whose grains are less refined. In the Fused Zone (FZ), the observed bainite promotes an increase in hardness when compared to HAZ. In the case of the welded joint with ER70S-6, in the FZ, there is a grain boundary ferrite that was not observed in the welded joint with ER110S-G, causing the hardness in the FZ of the sample welded with ER110S-G to be greater.

Other information obtained by SEM observation from metallography, illustrated in Figure 6 and 7, were:

- In the region of the base metal (BM), a place not affected by the welding process, a very fine microstructure was observed, characteristic of a complex phase steel, according to the literature (Mesplont, 2002), consisting of several phases, such as ferrite, constituent MA (retained austenite martensite) and bainite;



FZ - ER70S-6



ZF - ER110S-GFZ

Figure 6. Microstructures of the fused area (ZF) obtained by SEM, magnification of 5, 10 and 30 thousand times.

Copyright © 2019 ISESC.

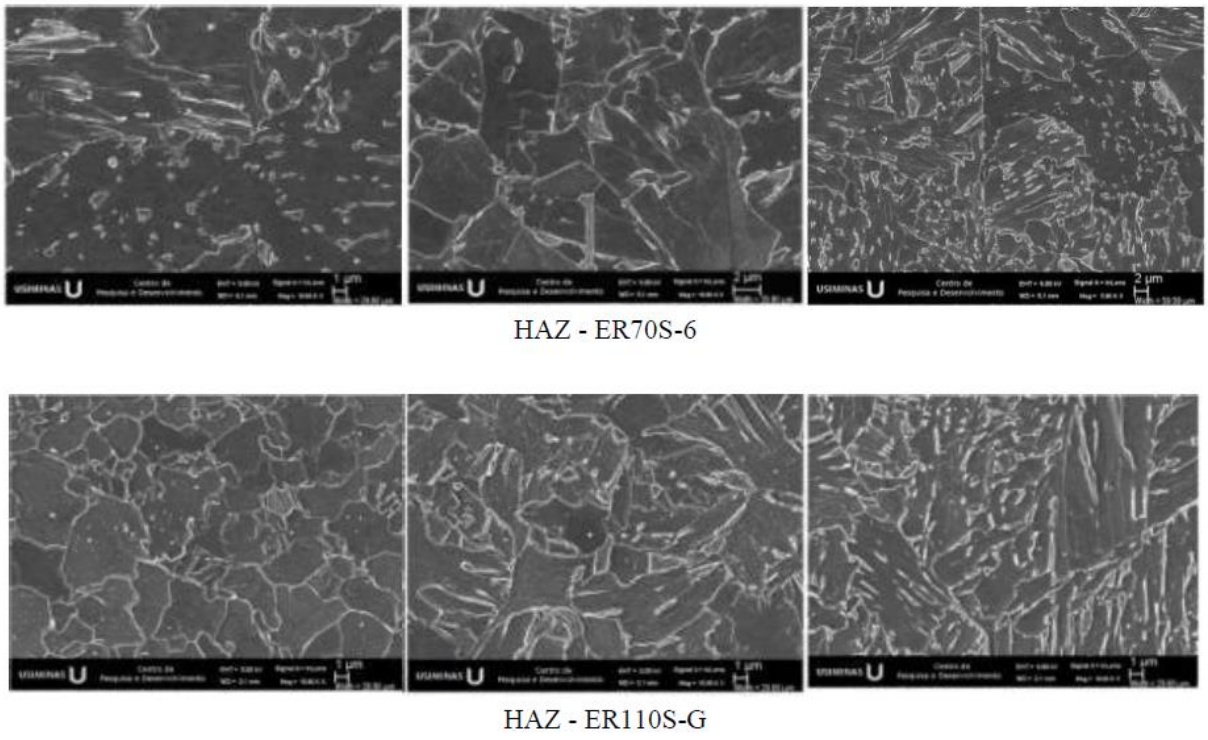


Figure 7. Microstructures of the hot affect zone (HAZ) obtained by SEM, magnification of 10 thousand times.

- In the region of the fused zone (FZ) of the welded joint obtained with ER110S-G consumable, only bainite was observed. In the FZ of the welded joint with ER70S-6, ferrite is observed. Figure 6 illustrates some of the metallographies registered at the FZ through SEM;

- In the HAZ of the welded joint with ER110S-G consumable, ferrite and a second phase in the microstructure are observed. In the subcritical region, a microstructure similar to that found in the base metal is observed, however, with larger ferrite grains. Due to this less refined microstructure than that of the base metal, there is a drop in hardness in this region when compared to the hardness obtained in USI-CP 800 steel (see Fig. 5);

- In the welded joint with the consumable ER70S-6, grain boundary ferrite, acicular ferrite and second phase ferrite were found, whereas in the coarse-grained region, ferrite with second phase aligned and non-aligned was found.

4. Conclusions

In this work, the robotized pulsed GMAW welding process was used to weld samples of the USI-CP 800 steel, hot rolled and tensile strength of 800 MPa. Considering the obtained results, it can be concluded that besides the resistance of the addition metal, other factors, such as the geometry of the weld, impact on the strength of the joint. The reduction of quantized hardness in the welded joint obtained with the ER110S-G consumable was less abrupt than the same reduction of this characteristic when analyzing the joint obtained with the ER70S-6 consumable. Therefore the increase in the mechanical resistance of the consumable used is beneficial for the maintenance of the mechanical strength of the joint as a whole and its structural continuity.

Acknowledgements

The authors gratefully acknowledge the collaboration and support in the development of this work from Inspebras; the execution of the robotic welding of the samples by Fronius Brasil; the specification and suppling of welding consumables by Voestalpine Böhler Welding Soldas do Brasil, and the test results furnished by USIMINAS-Cubatão Laboratory.

Copyright © 2019 ISESC.

References

ASTM A370-17. Standard Test Methods and Definitions for Mechanical Testing of Steel Products. The American Society for Testing and Materials. ASTM. 2017

AWS D1.1/D1.1M., 2015. Structural Welding CodeSteel. An American National Standard. *American Welding Society*. 23rd Edition. July 28, 2015.

AWS A5.18/A5.18M, 2001. Specification for carbon steel electrodes and rods for gas shielded arc welding. An American National Standard. *American Welding Society*. February 5, 2001.

AWS A5.28/A5.28M, 2005. Specification for low-alloy steel electrodes and rods for gas shielded arc welding. An American National Standard. *American Welding Society*. 3rd Edition. March 9, 2005.

Böhler, 2017. "Consumíveis para Solda de União" (Union Welding Consumables). Böhler Welding by Voestalpine. Aug. 2017 < http://www.voestalpine.com/welding/br/Servicos/Downloads>.

Burns, T. J., 2009. Weldability of a Dual-Phase Sheet Steel by the Gas Metal Arc Welding Process. M.Sc. thesis, University of Waterloo. Canada.

Cardenas, C.; Hernandez, L.; Tijerina, J. T. 2015. Effects of GMAW conditions on the tensile properties of hot rolled Complex Phase 780 steel. In *Proceedings of the Great Designs in Steel Seminar - GDSI 2015*, Detroid, USA.

EN 10338, 2015. Hot rolled and cold rolled non-coated products of multiphase steels for cold forming - Technical delivery conditions. *European Standard*. Bruxels, Belgium.

Ferreira, J.L. "Aspectos sobre a Estampagem dos Aços Utilizados pela Indústria Automotiva". Relatório "Aços para a Indústria Automotiva". Centro de Pesquisa e Desenvolvimento. USIMINAS. 19 de novembro de 2016

Kapustka, N; Conrardy, C.; Babu, S.; Albright, C., 2008. "Effect of GMAW Process and Material Conditions on DP 780 and TRIP 780 Welds. *Supplement to the Welding Journal (AWS / WRC)*. Vol. 87, pp. 135–148.

Keeler, S., Kimchi, M., Mooney, P.J., 2015. Advanced high strength steel application guidelines. Version 6.0. WorldAutoSteel. Mar. 2019 < https://www.worldautosteel.org/projects/advanced-high-strength-steel-application-guidelines/>.

Marra, K.M., 2008. "Aços Dual Phase da Usiminas: Características e Potencial de Aplicação em Veículos Automotores".In *Anais do 63º Congresso Anual da ABM*. Santos, Brazil.

Mesplont, C., 2002. Phase transformations and microstructure - mechanical properties relations in Complex Phase high strength steels. *Ingénieur Ecole Universitaire Des Ingénieurs de Lille. DEA Science des Matériaux*. Out. 2018 < http://hdl.handle.net/1854/LU-522033 >.

Copyright © 2019 ISESC.